Journal of Visualized Experiments

Key procedures to optimize sealing process and achieve real time monitoring
--Manuscript Draft--

Article Type:	Invited Methods Article - JoVE Produced Video
Manuscript Number:	JoVE60064R3
Full Title:	Key procedures to optimize sealing process and achieve real time monitoring
Keywords:	Residual stress, fiber Bragg grating, metal-to-glass seal, on-line monitoring, thermal and pressure loads.
Corresponding Author:	He Yan Tsinghua University Beijing, Beijing CHINA
Corresponding Author's Institution:	Tsinghua University
Corresponding Author E-Mail:	yanhe@mail.tsinghua.edu.cn
Order of Authors:	Zhichun Fan
	Kangjia Hu
	Zhiyong Huang
	Yong Zhang
	He Yan
Additional Information:	
Question	Response
Please indicate whether this article will be Standard Access or Open Access.	Standard Access (US$2,400)
Please indicate the **city, state/province, and country** where this article will be **filmed**. Please do not use abbreviations.	Beijing, China

1 **TITLE:**

2 Optimized Sealing Process and Real-Time Monitoring of Glass-to-Metal Seal Structures

3

4 **AUTHORS & AFFILIATIONS:**

5 Zhichun Fan[1], Kangjia Hu[2], Zhiyong Huang[1], Yong Zhang[2], He Yan[1]

6

7 [1]Institute of Nuclear and New Energy Technology, Key Laboratory of Advanced Reactor
8 Engineering and Safety of Ministry of Education, Collaborative Innovation Center for Advanced
9 Nuclear Energy Technology, Tsinghua University, Beijing, China
10 [2]Institute of Nuclear and New Energy Technology, Beijing Key Laboratory of Fine Ceramics,
11 Tsinghua University, Beijing, China

12

13 **Corresponding Author:**

14 He Yan   (yanhe@tsinghua.edu.cn)

15

16 **E-mail Addresses of Co-authors:**

17 Zhichun Fan: (fzc16@mails.tsinghua.edu.cn)
18 Kangjia Hu: (hkj17@mails.tsinghua.edu.cn)
19 Zhiyong Huang: (huangzy@tsinghua.edu.cn)
20 Yong Zhang: (yzhang@tsinghua.edu.cn)

21

22 **KEYWORDS:**

23 residual stress, fiber Bragg grating, metal-to-glass seal, online monitoring, thermal load, pressure
24 load, MTGS

25

26 **SUMMARY:**

27 Key procedures to optimize the sealing process and achieve real-time monitoring of the metal-
28 to-glass seal (MTGS) structure are described in detail. The embedded fiber Bragg grating (FBG)
29 sensor is designed to achieve online monitoring of temperature and high-level residual stress in
30 the MTGS with simultaneous environmental pressure monitoring.

31

32 **ABSTRACT:**

33 Residual stress is an essential factor to keeping the hermeticity and robustness of a glass-to-metal
34 seal structure. The purpose of this report is to demonstrate a novel protocol to characterize and
35 measure residual stress in a glass-to-metal seal structure without destroying the insulation and
36 hermeticity of sealing materials. In this research, a femto-laser inscribed fiber Bragg grating
37 sensor is used. The glass-to-metal seal structure that is measured consists of a metal shell, sealing
38 glass, and Kovar conductor. To make the measurements worthwhile, the specific heat treatment
39 of metal-to-glass seal (MTGS) structure is explored to obtain the model with best hermeticity.
40 Then, the FBG sensor is embedded into the path of sealing glass and becomes well-fused with
41 the glass as the temperature cools to RT. The Bragg wavelength of FBG shifts with the residual
42 stress generated in sealing the glass. To calculate the residual stress, the relationship between
43 Bragg wavelength shift and strain is applied, and the finite element method is also used to make
44 the results reliable. The online monitoring experiments of residual stress in sealing glass are

45 carried out at different loads, such as high temperature and high pressure, to broaden functions
46 of this protocol in harsh environments.
47
48 **INTRODUCTION:**
49
50 Metal-to-glass sealing is a sophisticated technology that combines interdisciplinary knowledge
51 (i.e., mechanics, materials, and electrical engineering) and is widely applied in aerospace[1],
52 nuclear energy[2], and biomedical applications[3]. It has unique advantages such as higher
53 temperature and pressure endurance compared with organic material sealing structures.
54 According to the difference of coefficient of thermal expansion (CTE), MTGS can be divided into
55 two types: matched seal and mismatched seal[4]. As for the matched seal, the CTE of metal (α_{metal})
56 and sealing glass (α_{glass}) are nearly the same to reduce the thermal stress in sealing materials.
57 However, to keep good hermeticity and mechanical robustness of the seal structure in harsh
58 environments (i.e., high temperature and high pressure), the mismatched seal displays better
59 performance than the matched seal. Due to the difference between α_{metal} and α_{glass}, the residual
60 stress generates in sealing glass after the annealing process of MTGS structure. If the residual
61 stress is too large (even exceeding the threshold value), the sealing glass displays small defects,
62 such as cracks. If the residual stress is too small, the sealing glass loses its hermeticity. As a result,
63 the value of residual stress is an important measurement.
64
65 Analysis of residual stress in MTGS structures has aroused research interests of many groups
66 around the world. The numerical model of axial and radial stress was built based on thin shell
67 theory[5]. The finite element method was applied to obtain the global stress distribution of an
68 MTGS structure after the annealing process, which was consistent with experimental results[6,7].
69 However, because of limitations involving small size and electromagnetic interference, many
70 advanced sensors are not suitable for these circumstances. The indentation crack length method
71 was reported to measure the residual stress in the sealing material of MTG; however, this method
72 was destructive and could not achieve real-time online monitoring of stress changes in glass.
73
74 Fiber Bragg grating (FBG) sensors are small in size (~100 μm) and resistant to electromagnetic
75 interference and harsh environments[8]. In addition, the components of the fiber are similar to
76 those of sealing glass (SiO_2), so FBG sensors have no effects on the hermeticity and insulation of
77 the sealing material. FBG sensors have been applied to the residual stress measurement in
78 composite structures[9-11], and results showed that it displayed good measuring precision and
79 signal response. Simultaneous temperature and stress measurements may be achieved by fiber
80 Bragg grating arrays on one optical fiber[12,13].
81
82 A novel protocol based on an FBG sensor is demonstrated in this study. The appropriate
83 preparation for the special MTGS structure has been explored by adjusting the maximum heat
84 temperature to ensure the good hermeticity of the MTGS structure. The FBG sensor is embedded
85 in the prepared path of sealing glass to fuse the FBG and glass together after the heat treatment.
86 Then, the residual stress can be obtained by the Bragg wavelength shift of the FBG. The MTGS
87 structure with the FBG sensor is placed under high temperature and high pressure environments
88 to achieve online monitoring of residual stress under changing loads. In this study, the detailed

89 steps to produce an MTS structure with a FBG sensor are outlined. The results show the feasibility
90 of this novel protocol and establish the foundation for the failure diagnosis of an MTGS structure.
91
92 **PROTOCOL:**
93
94 **1. Production of MTGS structure with good hermeticity**
95
96 NOTE: The procedures for MTGS structure include the preparations for components of the
97 combined structure, the heat treatment process, and examinations for the performance of MTGS
98 samples. The complete MTGS structure consists of a steel shell, Kovar conductor, and sealing glass.
99 See the diagram and dimensions shown in **Figure 1** and **Table 1,** respectively.
100
101 1.1 Pour the granulated glass powder (~1.1 g) into the mold, then place the mold onto the press
102 machine to process the granulated glass as shown in **Figure 2a,b,b**.
103
104 1.2 Switch on the press machine (push the red button) to compact the granulated glass into the
105 glass cylinder as shown in **Figure 2c,d**.
106
107 NOTE: The density control of glass cylinder is important for the performance of the MTGS
108 structure, because too many pores in the glass cylinder will lead to failure of the hermeticity of
109 MTGS structure.
110
111 1.3 Place the glass cylinder into the heating furnace to be sintered (see **Figure 3)**.
112
113 1.4 The sintered glass cylinder, steel shell, and Kovar conductor are manufactured with a special
114 graphite gasket, as shown in **Figure 4a**. Place this model onto the quartz septum in the heating
115 furnace using a claw for heat treatment (see **Figure 4b**). Keep the cooling rate as 0.5 °C/min to
116 avoid breaking of the optical fiber.
117
118 1.5 Use visual inspection to identify the surface topography of sealing glass after retrieving the
119 model from the heating furnace.
120
121 1.6 Use the high pressure pipeline to examine the hermeticity of MTGS model. Install the model
122 onto the pipeline by the card sleeve type joint. Slowly change the pressure from 1 MPa to 8 MPa,
123 holding each pressure for 24 h.
124
125 1.7 Use the scanning electron microscope (SEM) to identify the microscopic interface between
126 sealing glass and metal parts as shown in **Figure 5**. Use 15 kV and 500x magnification to observe
127 the interface clearly.
128
129 NOTE: From the macrography examination and SEM results, the standard maximum heating
130 temperature is set as 450 °C to obtain the MTGS model with good hermeticity. The standard
131 heating treatment is defined as follows: increase the temperature from (room temperature) RT
132 to 450 °C in increments of 5 °C/min, then drop the temperature to RT as 0.5 °C/min.

133

2. Residual stress measurement in sealing glass

NOTE: The FBG sensor is designed as an appropriate method to measure the stress in the MTGS. The grating length of the FBG sensor is 5 mm to match the height of the glass (5 mm) well.

2.1 Compact the granulated glass powder into the glass cylinder as described in steps 1.1–1.2.

NOTE: The height of glass cylinder is important, because if the cylinder is too high (>6 mm), it will be difficult to make a through path for the FBG sensor without destroying the glass material.

2.2 Drill the glass cylinder using drill speed of 5,000 rpm to produce three equally spaced through-holes to prepare paths for optical fiber sensors (diameter 0.45 mm). Sinter the glass cylinder with holes using the same heat treatment as shown in **Figure 4**.

2.3 Manufacture the MTGS model as described in step 1.4. Then, put the fiber through the path in sealing glass and position the grating region of the FBG exactly within the glass.

NOTE: Because the flow in the vertical furnace can blow up the grating region, which leads to the mismatching of FBG and glass, the tail of optical fiber must be hung with a small nail to keep the position of FBG accurate.

2.4 Fuse the head of optical fiber with a FC connector by the fusion splicers. Then, match the FC connector with the OPM-T400, which is an interrogator to demodulate the wavelength data and spectrum of FBG. The OPM-T400 is connected to a computer, and the supporting software on the computer can obtain experimental data.

2.5 Process the whole model in a furnace by the standard heat treatment obtained previously. Raise the temperature from RT to 450 °C as 5 °C/min, then drop the temperature to RT in increments of 0.5 °C/min. The grating region will become fused with the sealing glass as it is heated to melt. When the temperature cools down to RT, the glass will solidify and the FBG sensor will become well-fused with the sealing material.

2.6 Record the real-time Bragg wavelength data using the software (shown in **Figure 6**). The only factor inducing changes of wavelength and spectrum is the residual stress generated in sealing glass, because the temperature before and after this step is both RT.

NOTE: The residual stress can be calculated through the strain-wavelength relationship of FBG[14] and Hook's law, as shown below.

$$\frac{\Delta\lambda_B}{\lambda_B} = (1 + P_e) \times \varepsilon$$

$$\sigma = E \times \varepsilon$$

Where: the $\Delta\lambda_B$ is the Bragg wavelength shift induced by the residual stress, λ_B is the initial

wavelength of FBG, P_e is the strain-optic coefficient, ε is the residual strain in the glass, E is the Young's modulus of sealing glass, and σ is the residual stress in the glass.

NOTE: When working at a high temperature, the hermeticity of the MTGS structure will be affected, because the thermal expansion of steel shell leads to the decrease of residual stress in sealing glass. Thus, it is possible this protocol can prevent the failure of hermeticity due to the online monitoring of residual stress change in sealing glass.

3.1 Manufacture the MTGS model as done in step 1.4. The type of FBG to monitor temperature and stress simultaneously is the fiber Bragg grating array sensor, including two grating regions on one fiber, with a 10 mm distance between these two sensors.

NOTE: These two grating are defined as FBG-1 and FBG-2. The initial Bragg wavelengths of FBG-1 and FBG-2 are 1545 nm and 1550 nm, respectively.

3.2 Place FBG-1 into the sintered glass cylinder to monitor the stress and temperature. Place FBG-2 outside the glass to monitor the temperature only, as shown in **Figure 7b**. In this way, FBG-1 is affected by both temperature and residual stress change, and FBG-2 is only affected by temperature of sealing glass.

3.3 Place the MTGS model with optical fiber in the furnace as described in steps 2.2–2.3. Use the standard heat treatment to process the MTGS model with an embedded FBG sensor.

3.4 Impose temperatures of 100 °C, 200 °C, 300 °C, and 400 °C onto the model and hold each temperature for 100 min.

NOTE: FBG-1 monitors the stress and temperature simultaneously expressed as the Bragg wavelength shift $\Delta\lambda_{B-1}$, and FBG-2 monitors the temperature change by $\Delta\lambda_{B-2}$ as shown in **Figure 8**. The relationships between Bragg wavelength shift and measured parameters are shown as follows:

$$\frac{\Delta\lambda_{B-1}}{\lambda_{B-1}} = (1 + P_e) \times \varepsilon + (\xi + \alpha) \times \Delta T$$

$$\frac{\Delta\lambda_{B-2}}{\lambda_{B-2}} = (\alpha + \xi) \times \Delta T$$

Where: ξ is thermo-optic coefficient, α is thermal expansion coefficient of optical fiber, and ΔT is temperature change before and after the experiment. The $\Delta\lambda_{B-3}$ induced by residual stress can be separated through subtracting $\Delta\lambda_{B-1}$ from $\Delta\lambda_{B-2}$. This is the demodulation method for simultaneous temperature and stress monitoring of sealing glass at high temperatures.

4. Monitoring high pressure

217

218   NOTE: The pressure loads on the MTGS structure will have effects on the residual stress in sealing
219   glass, so the MTGS model with the embedded FBG sensor is a potential method to monitor the
220   high pressure change.

221

222   4.1 Prepare the same MTGS model with the FBG sensor as described in step 2.2–2.3. After the
223   FBG is well-fused with MTGS model, use the claw to take the model out of the furnace.

224

225   4.2 Manufacture the MTGS model with the FBG sensor onto a high pressure helium pipeline by
226   the bite type tube fittings as shown in **Figure 9**. Adjust the pressure from 1 MPa to 7 MPa by
227   pressure reducing the valve to impose changing pressure loads on the sealing structure.

228

229   4.3 The Bragg wavelength shift $\Delta\lambda_B$ is recorded as shown in **Figure 10**. At the same time, the
230   related residual stress change can be calculated using **Equation 1** and **Equation 2**.

231

232   **5. Theoretical analysis of MTGS structure**

233

234   5.1 Use the modeling software to build the 3D model for MTGS structure, and the dimensions are
235   taken from **Table 1** to keep the experimental model and theoretical model consistent.

236

237   5.2 Import the 3D model into the finite element analysis software. Assign mechanical properties
238   to the steel shell, sealing glass and Kovar conductor, as shown in **Table 2**.

239

240   5.3 The grid type of the whole model is Hex shape (see **Figure 11**). The mesh method of the
241   sealing glass and steel shell are sweep, and the Kovar conductor is meshed by structured method.
242   Refine the mesh of sealing glass to guarantee the accuracy of theoretical results. The elements
243   number of Kovar conductor, sealing glass and steel shell are 143700, 20350, and 13400,
244   respectively.

245

246   5.4 Set the initial increment, minimum increment, and maximum increment of the static analysis
247   step as 0.01, 1.00×10^{-8} and 1.00×10^{-2}, respectively.

248

249   5.5 Ensure that the interfaces between the sealing glass and metal parts are bounded. First,
250   impose the changing temperature load (from 370 °C to 20 °C) to simulate the solidification
251   progress of the MTGS model. The stress distribution after this process is shown in **Figure 12**.

252

253   5.6 Impose different temperatures (from 100 °C to 400 °C) onto the whole model to simulate the
254   online monitoring experiments under thermal loads. Under the other circumstance, changing
255   pressure loads (from 1 MPa to 7 MPa) are imposed on the sealing glass to simulate the online
256   monitoring under high pressure. The boundary conditions are shown in **Figure 13**.

257

258   5.7 The numerical results of stress and strain distribution of the whole model are obtained from
259   the destination file shown in **Figure 14**. Extract the analysis path in the sealing glass shown in
260   **Figure 13**, of which the position is the monitoring path for FBG sensors in **Figure 6a** to provide

261 comparison with the measuring results by FBG.
262
263 **REPRESENTATIVE RESULTS:**
264 From the results of **Figure 5**, the standard heat treatment to produce the MTGS models with high
265 pressure endurance is explored, and the models can satisfy the examinations (i.e., light
266 transmissions, pressure endurance, SEM, etc.). Thus, the produced MTGS structure can be applied
267 to keep hermeticity in harsh environments.
268
269 The FBG can be well-fused with MTGS structure, and the residual strain in sealing glass will be
270 reflected by Bragg wavelength shift after the heat treatment, as shown in **Figure 6**. The value of
271 residual stress can be calculated accurately using **Equation 1** and **Equation 2**. It is almost the same
272 as the results from the numerical simulation in **Figure 12**.
273
274 The real-time stress changes of sealing glass from 100 °C to 400 °C are monitored precisely by the
275 FBG sensor shown in **Figure 8**, and the decrease of residual stress in sealing glass can be reflected
276 instantaneously. It is necessary to keep the residual stress at a high level. As a result, the
277 preventions to keep the hermeticity of MTGS structure can be achieved using this protocol.
278
279 From the results of **Figure 10**, the real-time stress changes of sealing glass from 1 MPa to 7 MPa
280 are monitored sensitively, which maintains good consistency with the numerical results.
281 Therefore, the MTGS model with embedded FBG sensor is a potential sensor for high pressure
282 change monitoring.
283
284 **FIGURE LEGENDS:**
285
286 **Figure 1: Schematic diagram of the MTGS structure.** Three components are labeled.
287
288 **Figure 2: Manufacturing process for glass cylinder. (a)** The granulated low melting point sealing
289 glass. **(b)** The mold for glass powder. **(c)** Press machine to process glass powder into cylinder. **(d)**
290 The glass cylinder prepared for sintering.
291
292 **Figure 3: Sintered glass cylinder and related sinter treatment.** After the sinter process, the raw
293 glass material will turn into the sintered state for further process.
294
295 **Figure 4: MTGS structure and heat treatment to process MTGS structure. (a)** The manufactured
296 MTGS structure. **(b)** The detailed heat treatment that is divided into three stages according to
297 changes of sealing material. **(c)** The MTGS sample produced by the heat treatment.
298
299 **Figure 5: SEM and visual inspection of the MTGS samples produced with different performances.**
300 **(a)** Microstructure of sealing glass and steel shell with good hermeticity. **(b)** Smooth and glossy
301 surface of sealing glass with good hermeticity. **(c)** Microstructure of sealing glass and steel shell
302 with failed hermeticity. **(d)** Uneven surface of sealing glass with failed hermeticity.
303
304 **Figure 6: Residual stress measured by FBG. (a)** Set-up of three FBGs in the same sealing glass. **(b)**

305   Bragg wavelength curve during the sealing process with wavelength shift standing for residual
306   stress in the sealing glass.

307

308   **Figure 7: Simultaneous temperature and stress monitoring of MTGS structure by FBG arrays. (a)**
309   Photograph of the MTGS sample placed in the furnace. **(b)** Set-up of the online state monitoring
310   experiment under thermal load.

311

312   **Figure 8: Online monitoring results under thermal loads.** The top picture shows the signal
313   affected by stress and temperature change. The middle picture shows the temperature
314   monitoring signal. The bottom picture shows the stress monitoring signal.

315

316   **Figure 9: Online monitoring under pressure loads. (a)** Photograph of the high pressure pipeline.
317   **(b)** Set-up of the online state monitoring experiment under pressure load.

318

319   **Figure 10: Online state monitoring result of femto-laser inscribed FBG under pressure load.** The
320   wavelength of FBG sensor decreases almost linearly with the pressure increasing.

321

322   **Figure 11: Mesh of the MTGS structure with refinement of sealing glass.** The mesh from outside
323   to inside is respectively the steel shell, the sealing glass and the Kovar conductor.

324

325   **Figure 12: Numerical simulation of the MTGS structure after manufacturing process. (a)** Axial
326   stress and **(b)** radial stress vector graph of the sealing glass.

327

328   **Figure 13: Boundary conditions for online monitoring under thermal and pressure loads and**
329   **calculating paths.** The thermal loads change from 100 °C to 400 °C. The pressure loads change
330   from 1 MPa to 7 MPa. The axial path is exactly the measuring position of FBG in sealing glass.

331

332   **Figure 14: The version of software with destination files.** The special results (i.e., stress, strain,
333   etc.) can be extracted from this interface.

334

335   **Table 1: Dimensions of the MTGS structure.**

336

337   **Table 2: Mechanical properties of MTGS structure.**

338

339   **DISCUSSION:**
340   The critical steps for the stress measuring of sealing material of MTGS structure at high
341   temperature and high pressure include 1) manufacturing of the MTGS models with the FBG sensor,
342   of which the grating region is located at the middle of sealing glass; 2) heating of the whole model
343   using a standard heat treatment process, and after the model cools to RT, the FBG sensor will
344   becomes well-fused with MTGS model, and the residual stress can be measured by Bragg
345   wavelength shift; 3) placing of the complete model into the furnace to experience the changing
346   thermal loads, and the online simultaneous temperature and stress monitoring can then be
347   achieved by the wavelength shift difference of the two FBG arrays on one optical fiber; and 4)
348   manufacturing of the complete model onto a high pressure pipeline, and the stress change of

349 sealing glass with the varying pressure will be obtained by one single FBG in sealing glass.
350
351 Comparing the experimental and numerical results, the measured axial residual stress (56 MPa)
352 is almost the same as the theoretical value (53 MPa), and the residual stress change during the
353 online monitoring experiments under thermal and pressure loads agree with the simulation
354 results, with a deviation of less than 10%. This protocol is proved to be feasible and accurate
355 through FEM.
356
357 In the future, this protocol can be used to measure large-scale strain in an MTGS structure with
358 high melting point sealing glass (880 °C). The key issue in this experiment is the temperature
359 endurance of FBG sensor, so the type II grating inscribed by femto-laser point-to-point method
360 can be applied[15].
361
362 From the results of FEM, the strain distribution in sealing glass is non-uniform, which means that
363 the grating of FBG will be chirped and the spectrum broadened, clearly affected by the strain[16].
364 In the next steps, the relationship between the bandwidth of FBG and the strain distribution
365 should be studied, which can serve as a novel characterization to identify typical, non-uniform
366 strain induced by small cracks and other damage in the field of structural health monitoring[17-19].
367

371
372 **DISCLOSURES:**
373 The authors have nothing to disclose.
374

375 **REFERENCES:**
376 1.   Alves, F. J., Baptista, A. M., Marques, A. T. Metal and ceramic matrix composites in aerospace
377 engineering. *Advanced Composite Materials for Aerospace Engineering*. 59-99 (2016).
378 2.   Dai, S. et al. Sealing Glass-Ceramics with Near Linear Thermal Strain, Part I: Process
379 Development and Phase Identification. *Journal of the American Ceramic Society.* **99** (11), 3719-
380 3725 (2016).
381 3.   Karmakar, B. Glasses and glass-ceramics for biomedical applications. *Functional Glasses and
382 Glass-Ceramics*. 253-280 (2017).
383 4.   Shekoofa, O. et al. Analysis of residual stress for mismatch metal–glass seals in solar
384 evacuated tubes. *Solar Energy Materials and Solar Cells*. **128**, 421-426 (2014).
385 5.   Lei, D., Wang, Z., Li, J. The calculation and analysis of glass-to-metal sealing stress in solar
386 absorber tube. *Renewable Energy*. **35** (2), 405-411 (2010).
387 6.   Lei, D., Wang, Z., Li, J. The analysis of residual stress in glass-to-metal seals for solar receiver
388 tube. *Materials & Design*. **31**, 1813-1820 (2010).
389 7.   Dai, S. et al. Sealing glass-ceramics with near-linear thermal strain, part III: Stress modeling
390 of strain and strain rate matched glass-ceramic to metal seals. *Journal of the American Ceramic
391 Society*, **100** (8), 3652-3661 (2017).
392 8.   Hill, K. O., Meltz, G. Fiber Bragg grating technology fundamentals and overview. *Journal of

393   *Lightwave Technology*. **15** (8), 1263-1276 (1997).

394   9.   Prussak, P. et al. Evaluation of residual stress development in FRP-metal hybrids using fiber
395   Bragg grating sensors. *Production Engineering - Research and Development*. **12**, 259-267 (2018).

396   10.   Hu, H. et al. Investigation of non-uniform gelation effects on residual stresses of thick
397   laminates based on tailed FBG sensor. *Composite Structures*. **202**, 1361-1372 (2018).

398   11.   Colpo, F., Humbert, L., Botsis, J. Characterisation of residual stresses in a single fibre
399   composite with FBG sensor, *Composites Science & Technology*. **67** (9), 1830-1841 (2007).

400   12.   Jin, L. et al. An embedded FBG sensor for simultaneous measurement of stress and
401   temperature. *IEEE Photonics Technology Letters*. **18** (1), 154-156 (2005).

402   13.   Sampath, U. et al. Polymer-coated FBG sensor for simultaneous temperature and strain
403   monitoring in composite materials under cryogenic conditions. *Applied Optics*. **57** (3), 492-497
404   (2018).

405   14.   Kersey, A. et al. Fiber grating sensors. *Journal of Lightwave Technology*. **15** (8), 1442-1463
406   (1997).

407   15.   Mihailov, S. J. Fiber Bragg Grating Sensors for Harsh Environments. *Sensors*. **12** (12), 1898-
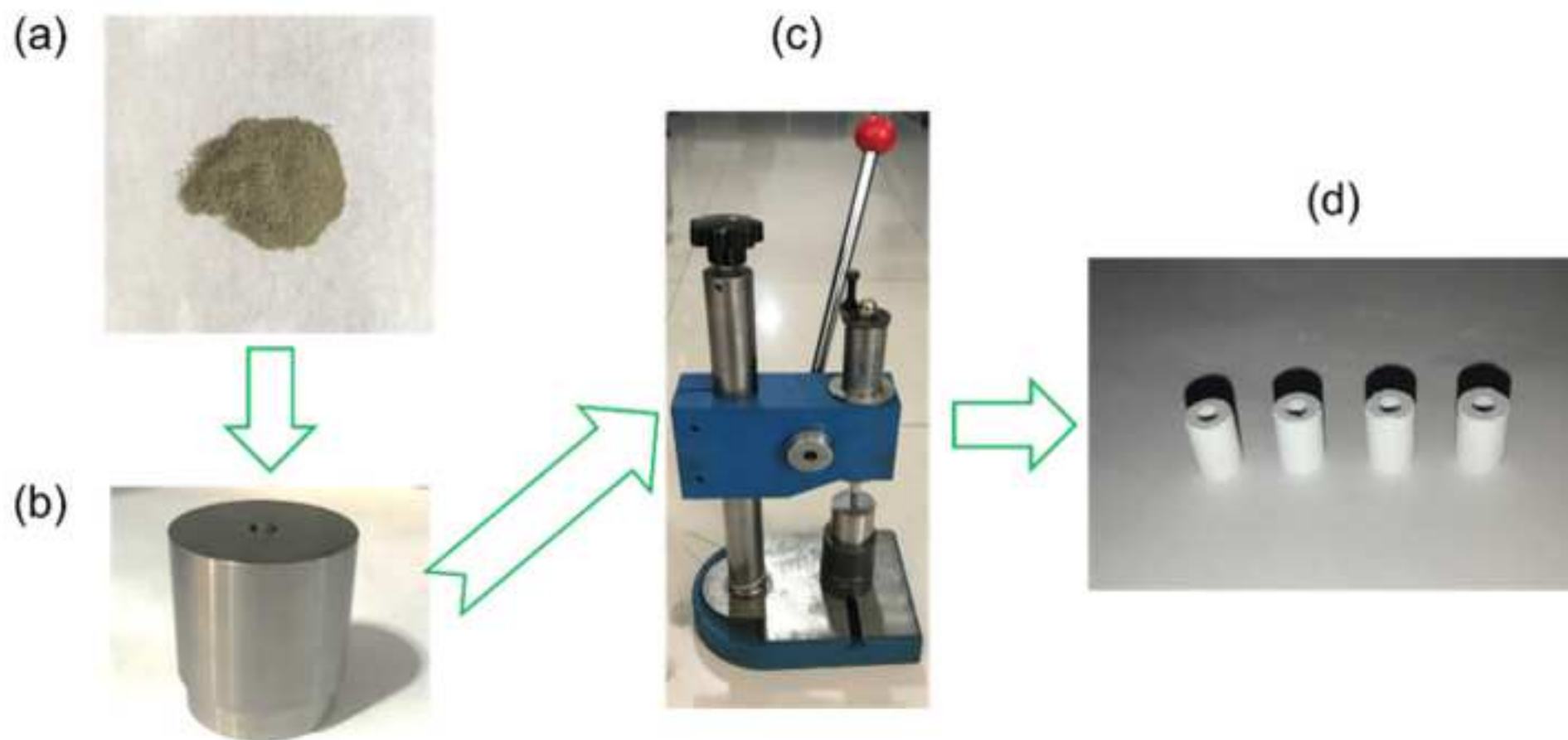408   1918 (2012).

409   16.   Morey, W. W., Meltz, G., Weiss, J. M. Recent advances in fiber-grating sensors for utility
410   industry applications. *Proceedings of SPIE - The International Society for Optical Engineering*. 90-
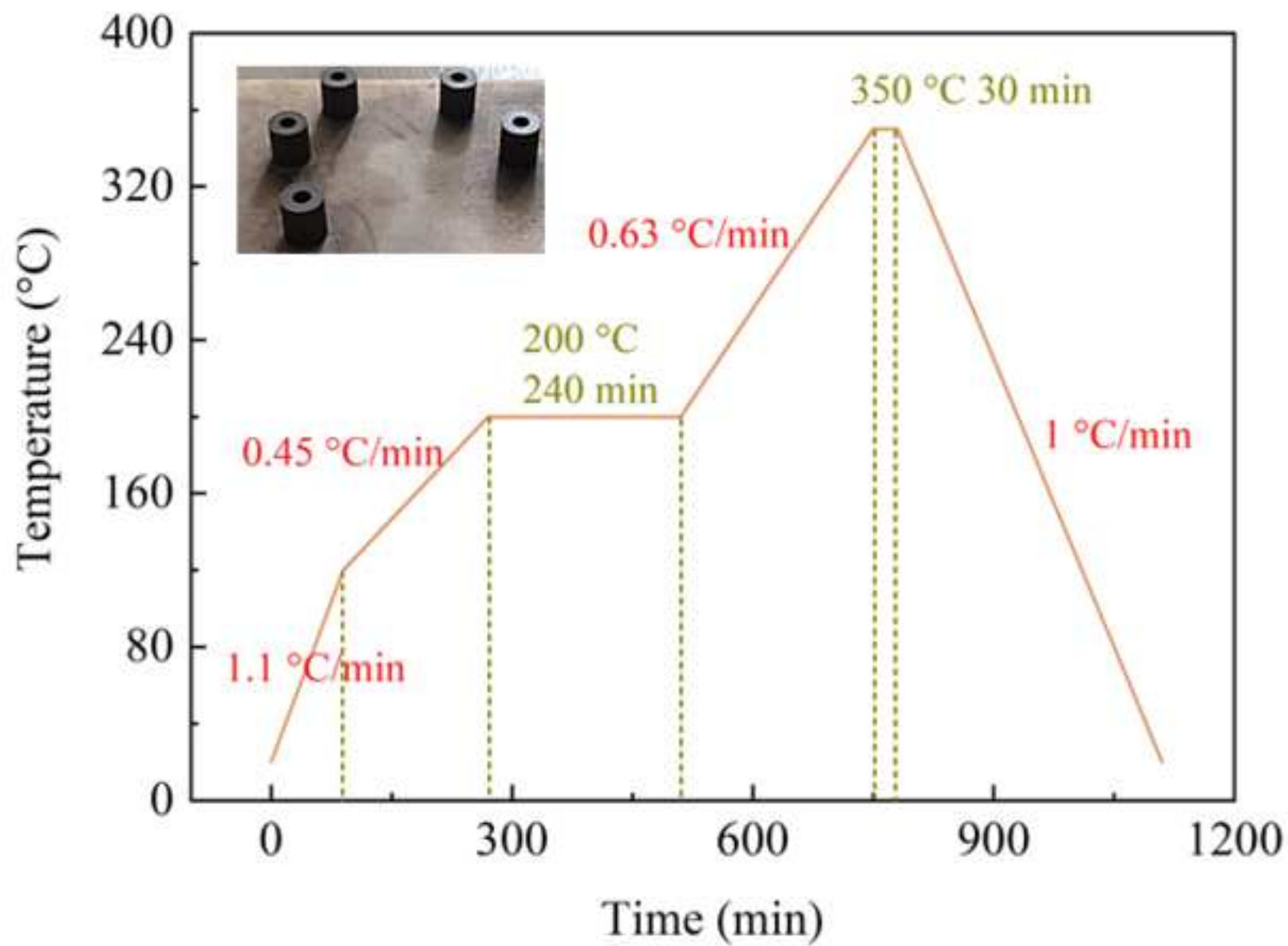411   98 (1996).

412   17.   Jin, X., Yuan, S., Chen, J. On crack propagation monitoring by using reflection spectra of AFBG
413   and UFBG sensors. *Sensors and Actuators A: Physical*. **285**, 491-500 (2019).

414   18.   Kakei, A. et al. Evaluation of delamination crack tip in woven fibre glass reinforced polymer
415   composite using FBG sensor spectra and thermo-elastic response. *Measurement*. **122**, 178-185
416   (2018).

417   19.   Zhang, W. et al. The Analysis of FBG Central Wavelength Variation with Crack Propagation
418   Based on a Self-Adaptive Multi-Peak Detection Algorithm. *Sensors*. **19** (5), 1056 (2019).
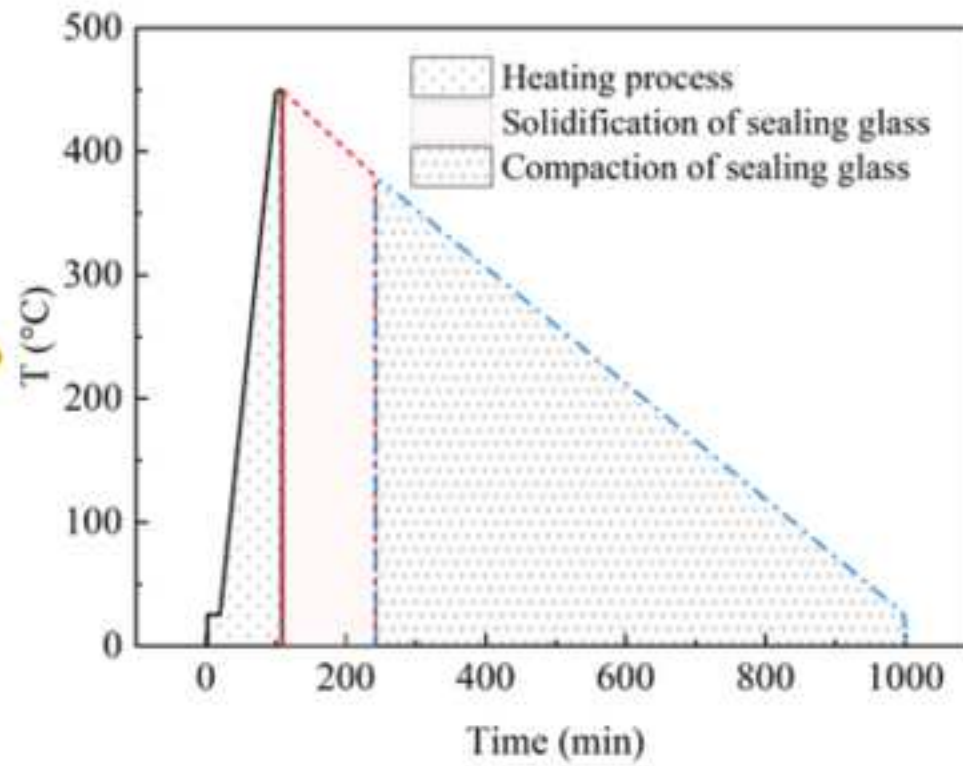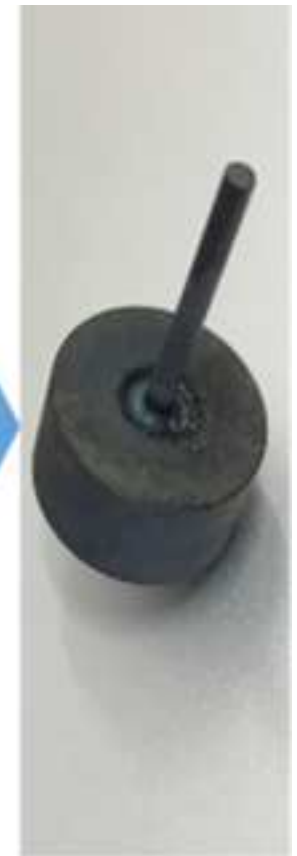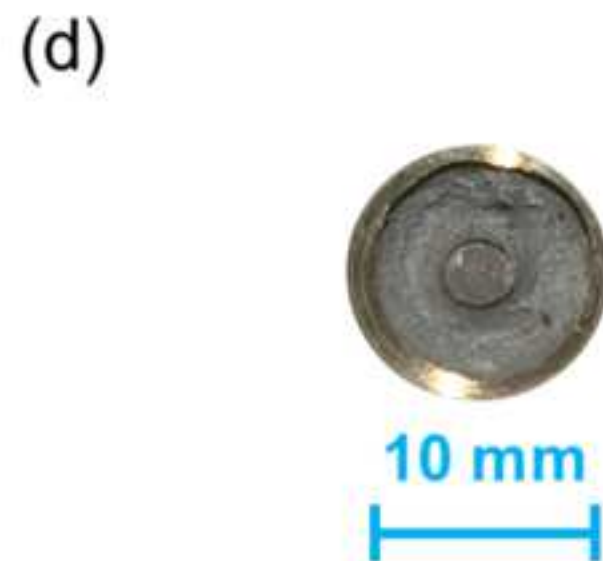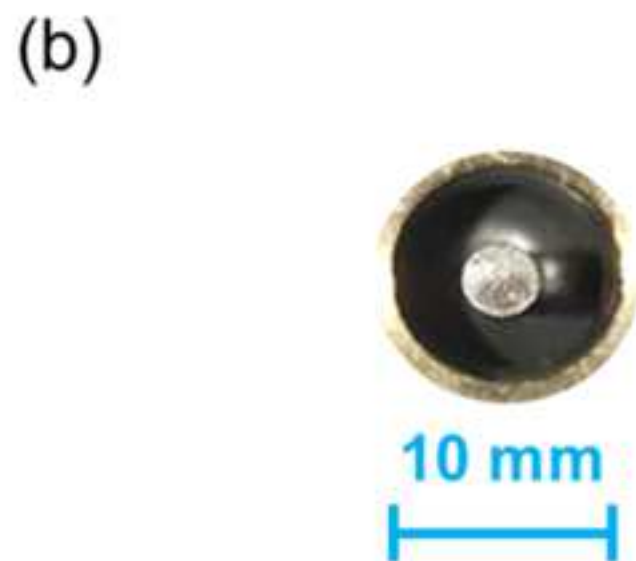
Figure1

Figure2   Click here to access/download;Figure;2.png

(a)

(b)

(c)

(d)

Figure3

Figure4

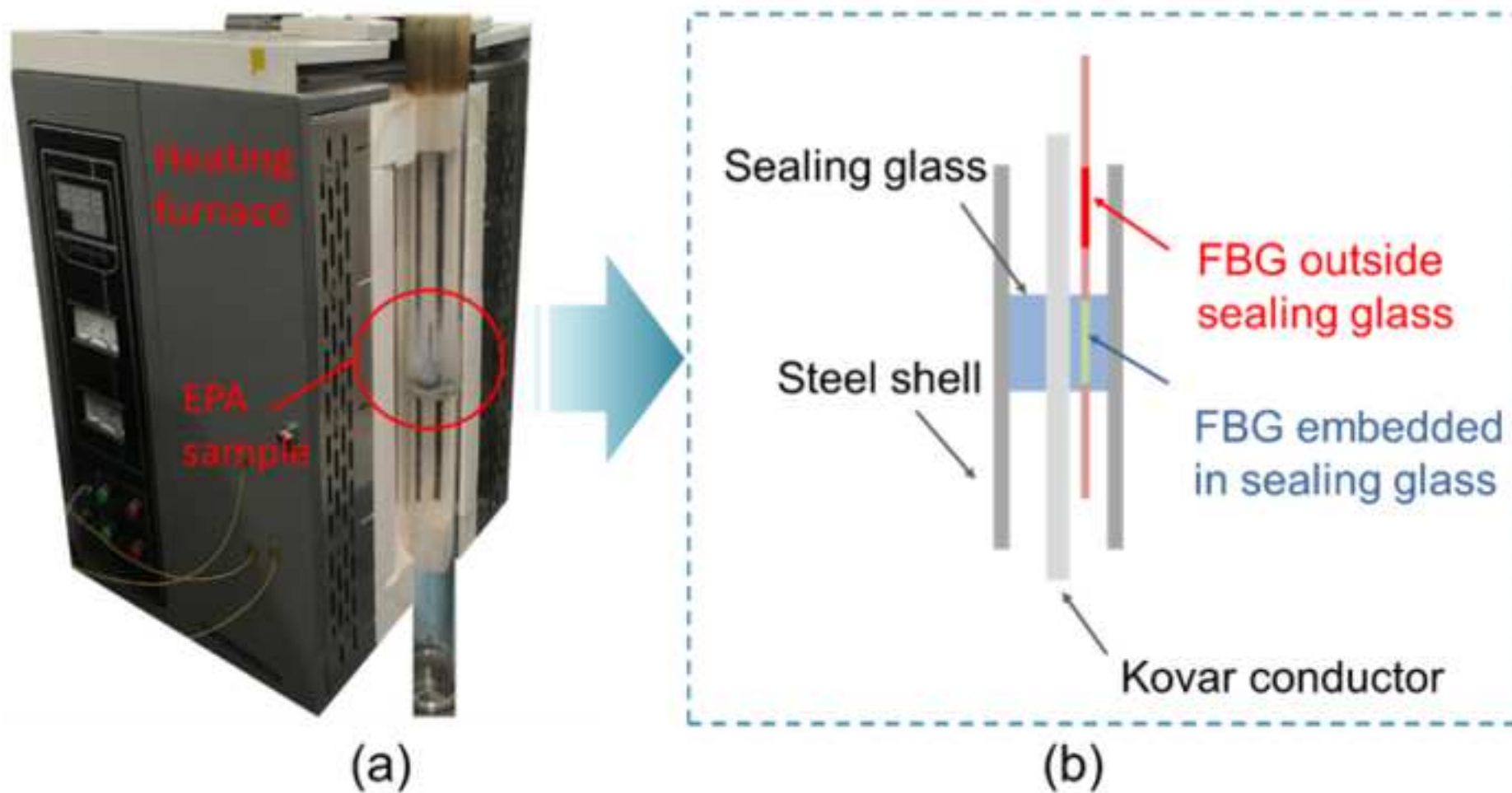(a)   (b)   (c)

Figure5
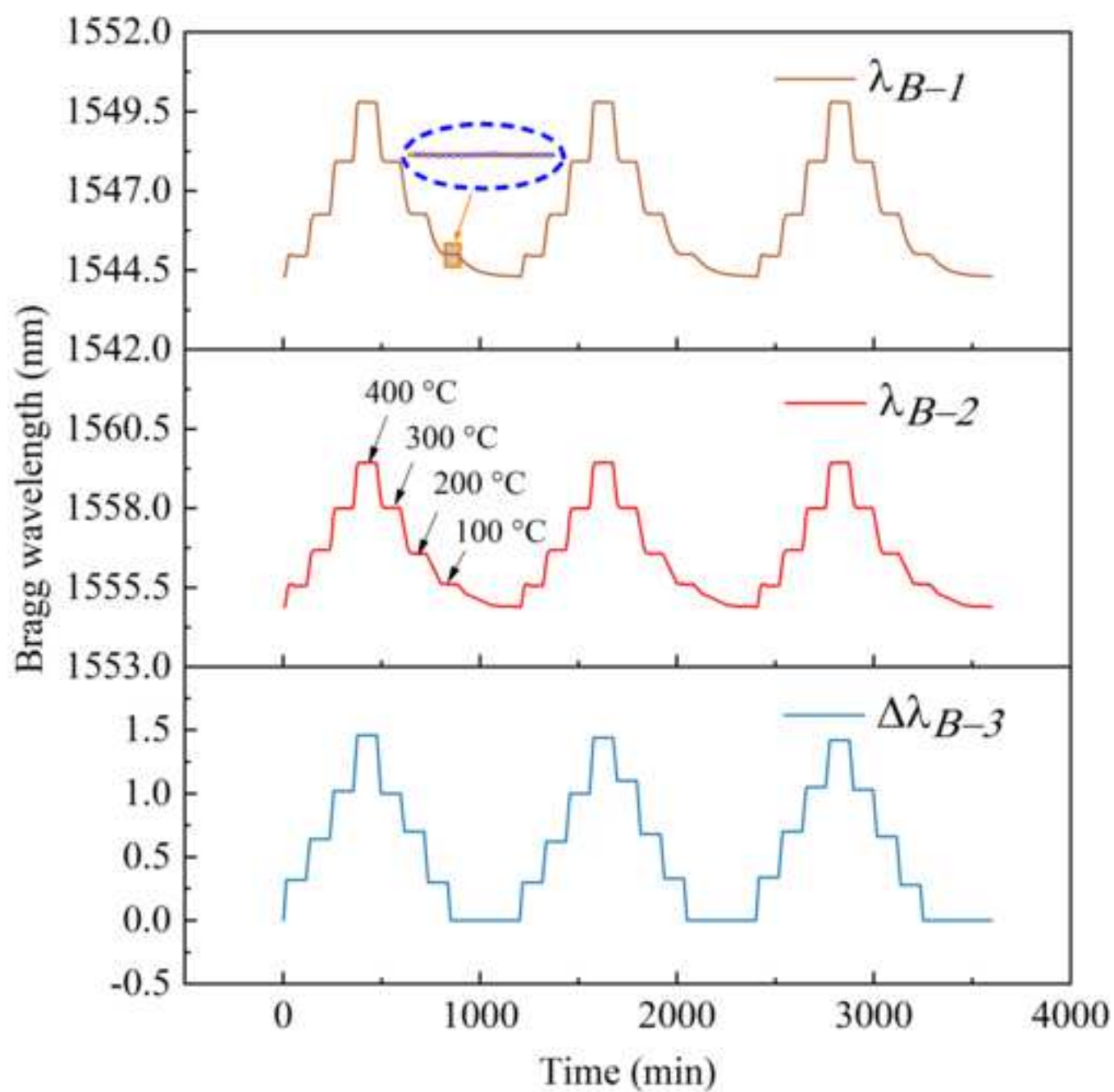
Figure6

Click here to access/download;Figure;6.png ⬇

(a)

Kovar conductor

Steel shell

FBG

Sealing

(b)

450 °C

$\Delta\lambda_{path1}=1.88$ nm

25 °C

$\Delta\lambda$

25 °C

Bragg wavelength (nm)

Time (min)

Figure7 Click here to access/download;Figure;7.png ⬇

(a)

Heating furnace

EPA sample

(b)

Sealing glass

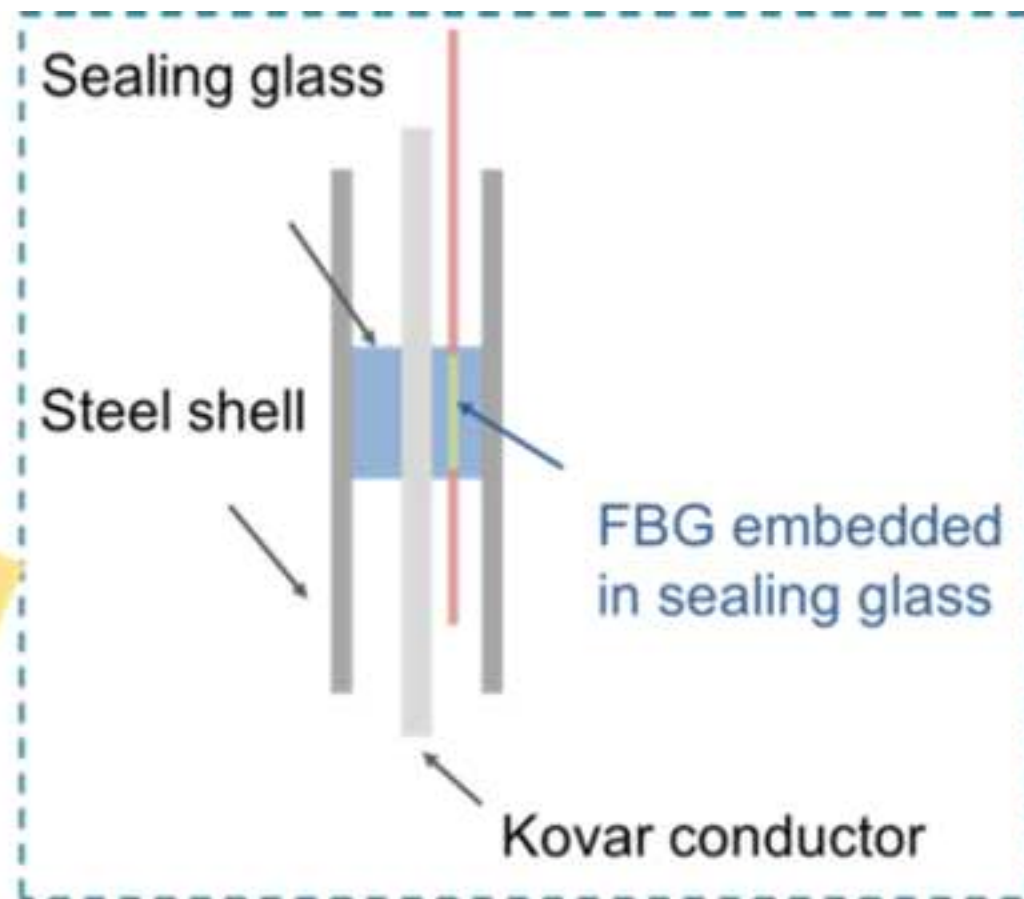Steel shell

FBG outside sealing glass

FBG embedded in sealing glass

Kovar conductor

Figure8

Click here to access/download;Figure;8.png ⬇
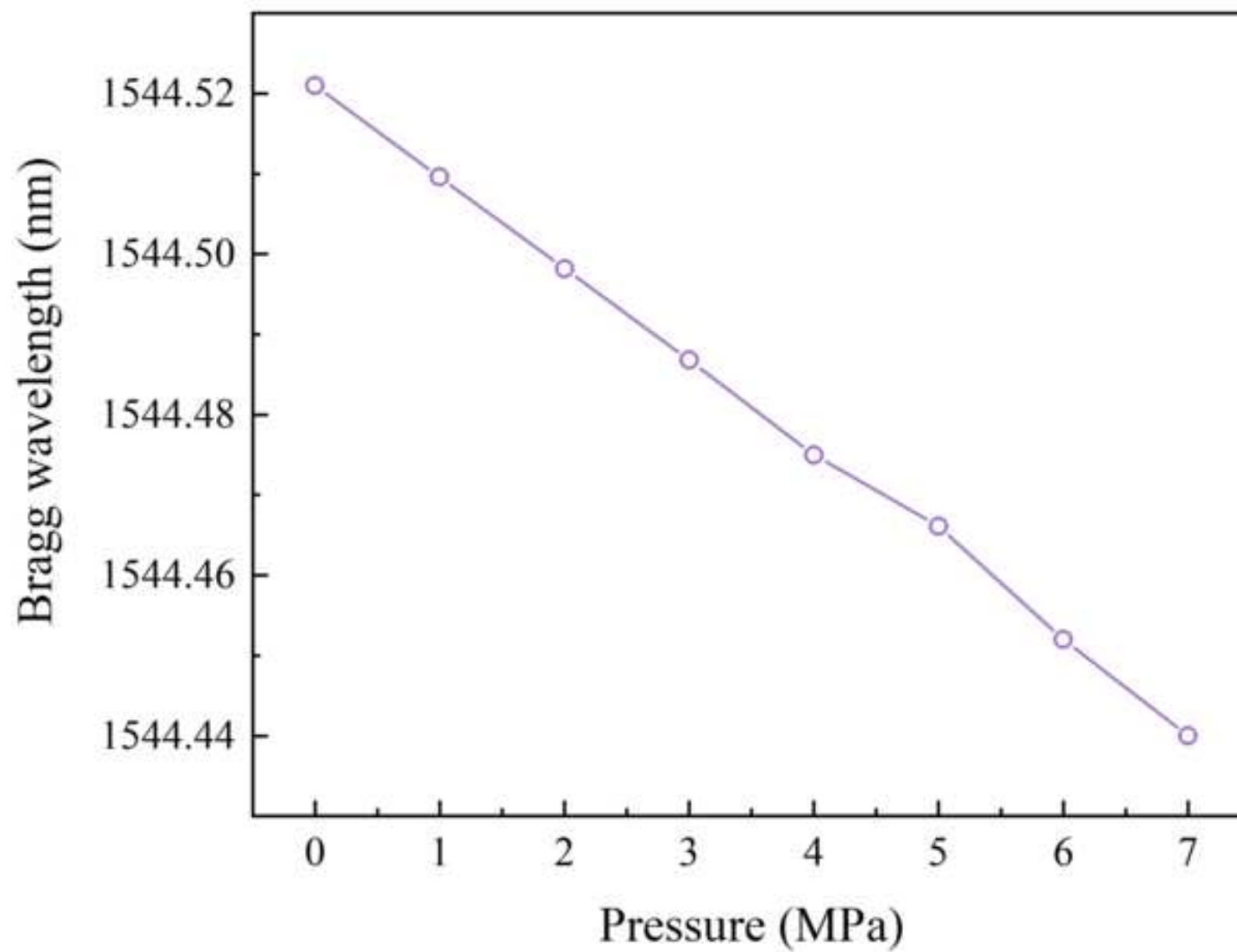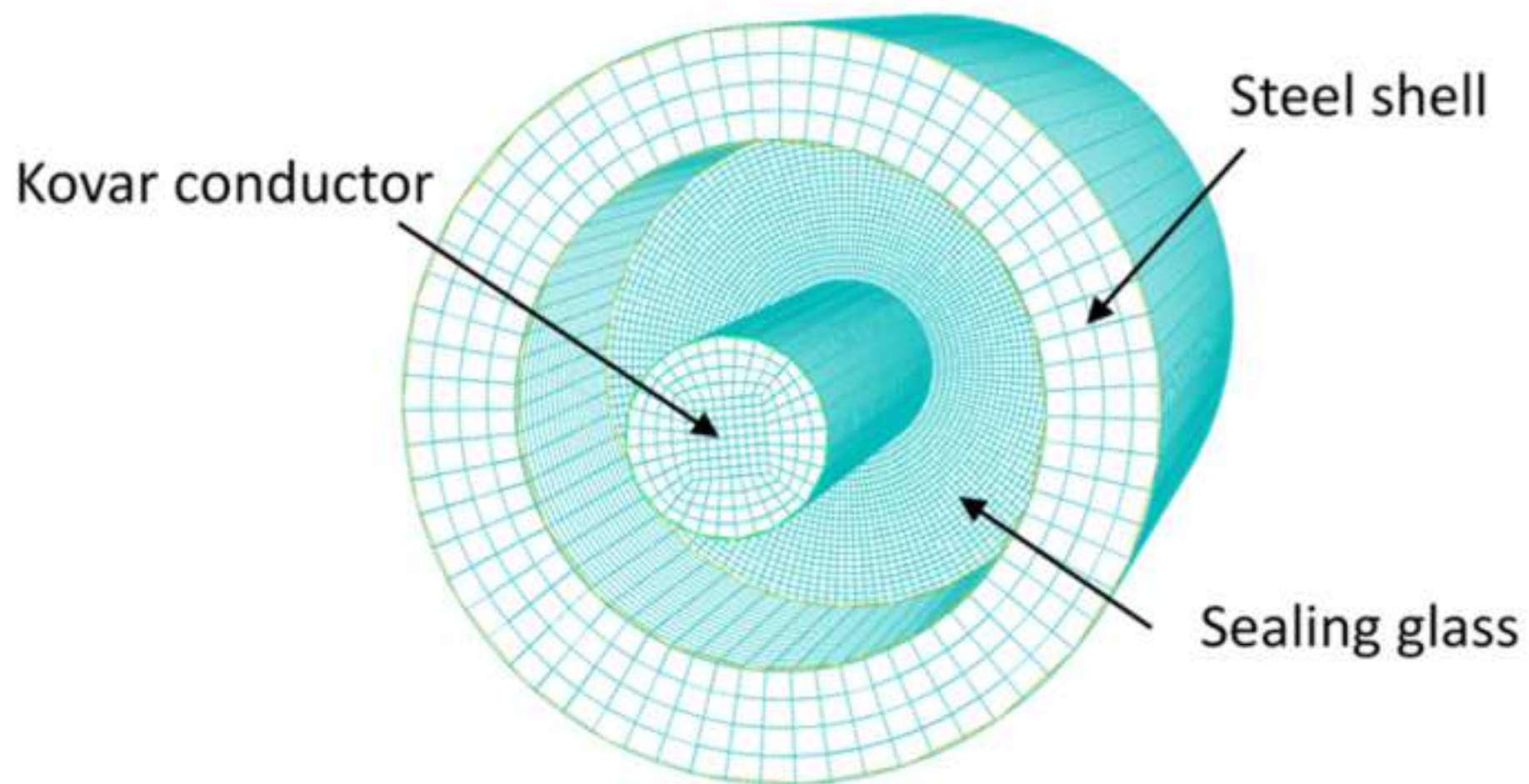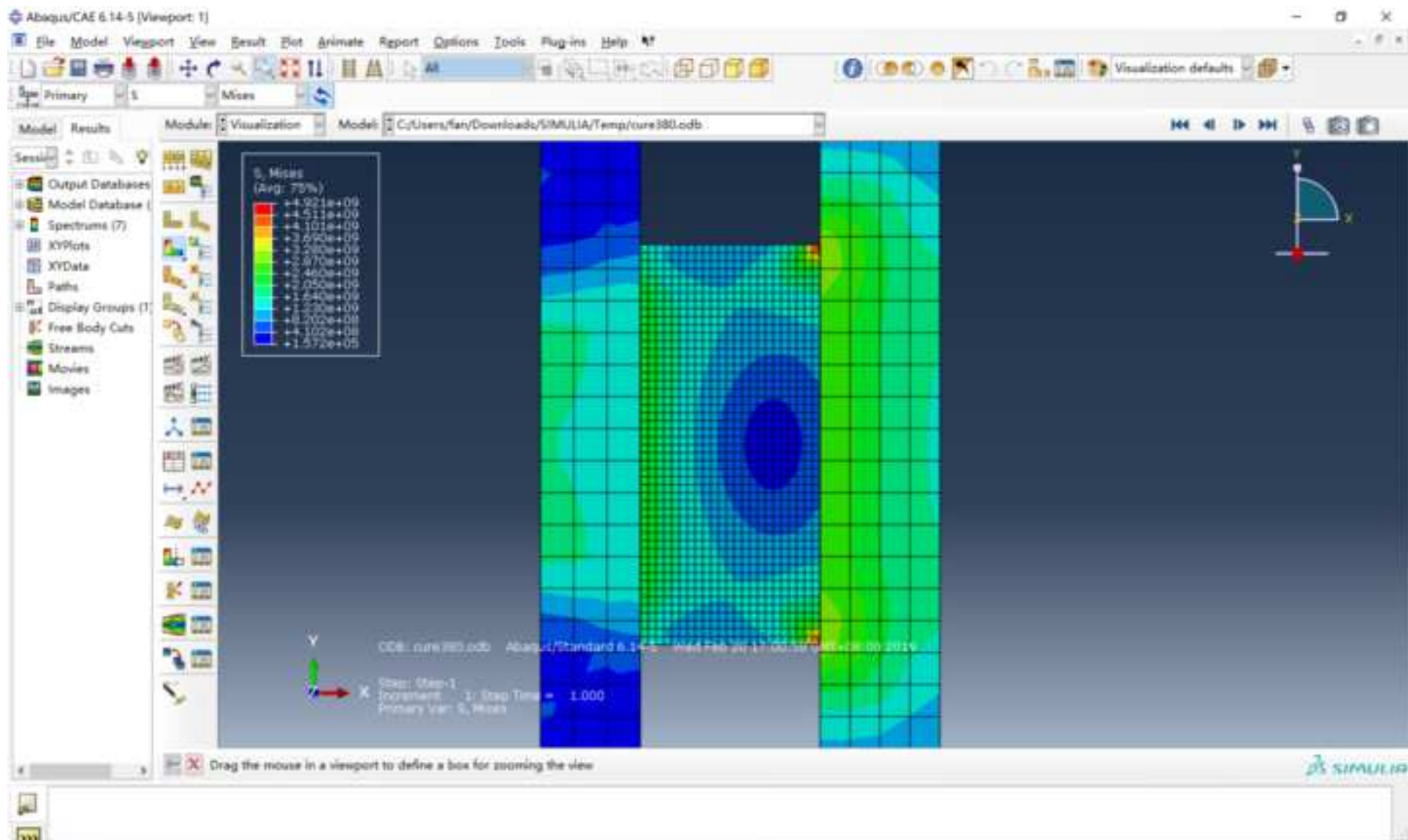
Figure9   Click here to access/download;Figure;9.png ⬇
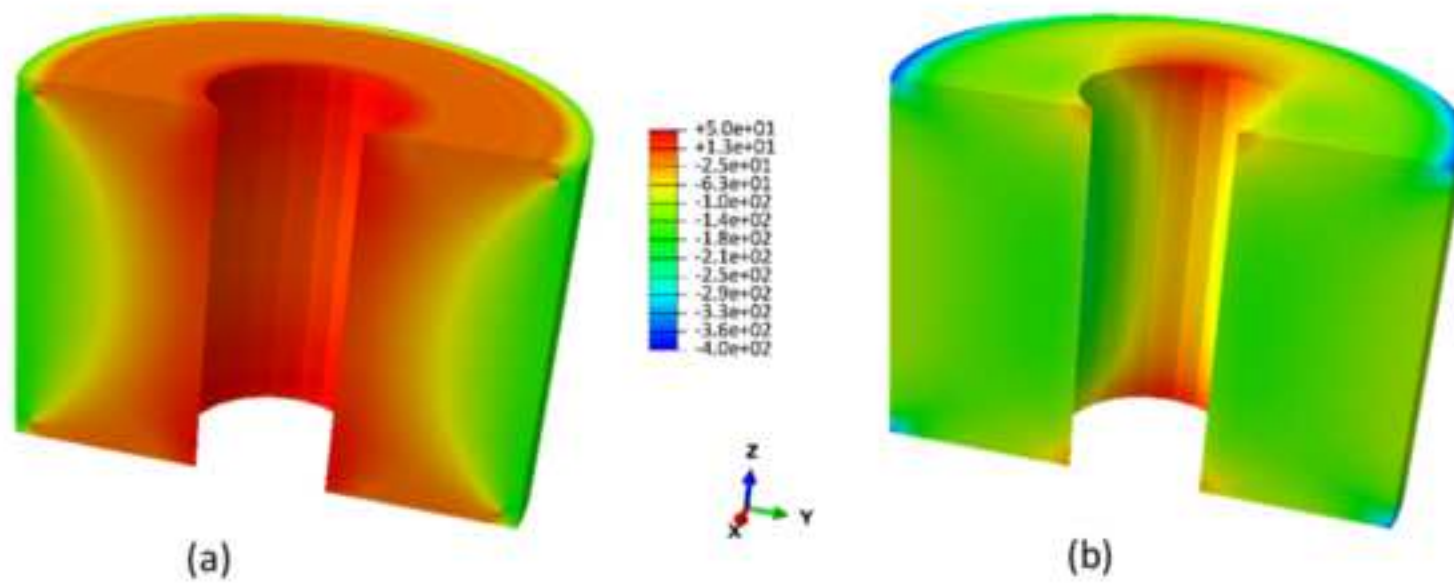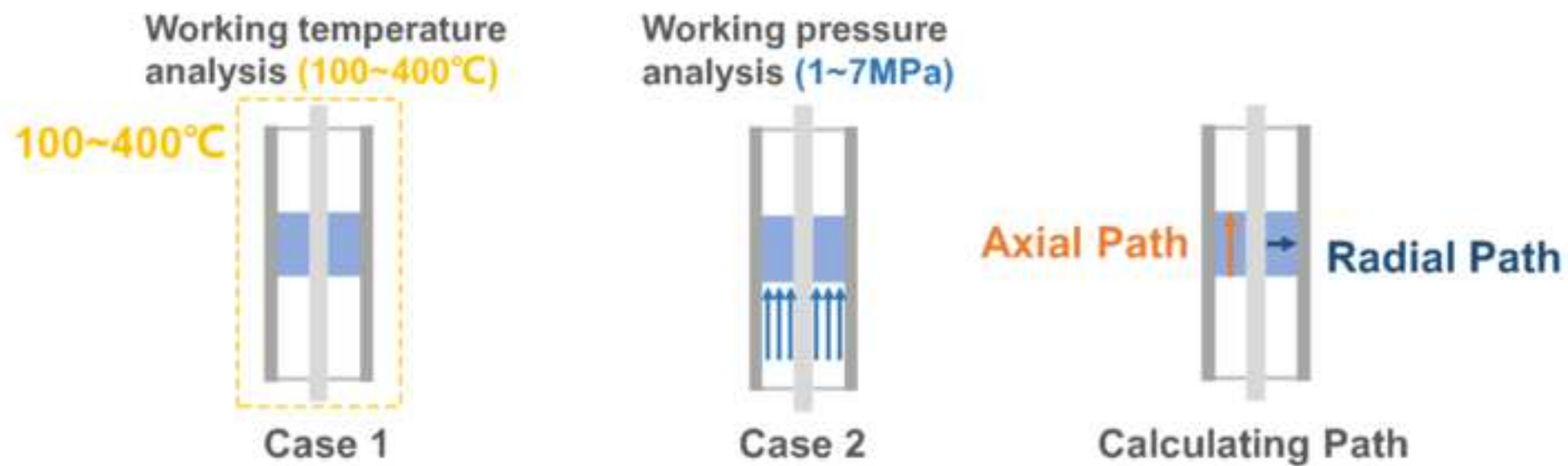

(a)   (b)

Figure10

Figure11

Steel shell

Kovar conductor

Sealing glass

Figure12

(a)

(b)

Figure13

Working temperature analysis (100~400°C)

100~400°C

Case 1

Working pressure analysis (1~7MPa)

Case 2

Axial Path   Radial Path

Calculating Path

Figure14

Table1

Dimensions (mm)	Steel shell	Sealing glass	Kovar conductor
Inner diameter	7	2.5	0
External diameter	10	7	2.5
Height	20	5	30

Dimensions (mm)	Steel shell	Sealing glass	Kovar conductor
Inner diameter	7	2.5	0
External diameter	10	7	2.5

Table2

Parameters	Steel shell	Sealing glass	Kovar conductor
Yong's modulus (GPa)	183	56.5	157
Poisson's ratio	0.3	0.25	0.3
Thermal expansion coefficient (1/°C)	1.6×10^{-5}	8.9×10^{-6}	4.9×10^{-6}

Parameters	Steel shell	Sealing glass	Kovar conductor
Yong's modulus (GPa)	183	56.5	157
Thermal expansion coefficient (1/°C)	1.6×10^{-5}	8.9×10^{-6}	4.9×10^{-6}

Name of Material/Equipment	Company	Catalog Number
ABAQUS	Dassault SIMULA	ABAQUS6.14-5
Fiber Bragg grating sensors	Femto Fiber Tec	FFT.FBG.S.00.02 Single
Fusion splicer	Furukawa Information Technologies and Telecommunications	S123M12
Glass powder	Shenzhen Sialom Advanced Materials Co.,Ltd	LC-1
Graphite mold	Machining workshop of Tsinghua University	Graphite
Heating furnace	Tianjin Zhonghuan Electric Furnace Technology Co., Ltd	SK-G08123-L
Kovar conductor	Shenzhen Thaistone Technology Co., Ltd	4J29
Optical interrogator	Wuhan Gaussian Optics CO.,LTD	OPM-T400
Pro/Engineer	Parametric Technology Corporation	PROE5.0
Steel shell	Beijing Xiongchuan Technology Co., Ltd	316 stainless steel

Comments/Description

The software to carry out numerical simulation.

apodized FBG

FITEL's line of fusion splicers provides an excellent solution for both field and factory splicing applications

A kind of low melting-point glass powder (380℃).

The mold to locate each part of the metal-to-glass structure.

vertical tubular furnace

A common material used for the electrical penetration in the metal-to-glass seal structure

FBG spectrum analysis modules

The software to establish the 3D geometry.

A kind of austenitic stainless steel

S。

jove

1 Alewife Center #200
Cambridge, MA 02140
tel. 617.945.9051
www.jove.com

JOURNAL OF VISUALIZED EXPERIMENTS

ARTICLE AND VIDEO LICENSE AGREEMENT

Title of Article: Key procedures to optimize sealing process and achieve real time monitoring

Author(s): Zhichun Fan, Kangjia Hu, Zhiyong Huang, Yong Zhang, He Yan.

Item 1: The Author elects to have the Materials be made available (as described at http://www.jove.com/publish) via:

[V] Standard Access   [ ] Open Access

Item 2: Please select one of the following items:

[V] The Author is **NOT** a United States government employee.

[ ] The Author is a United States government employee and the Materials were prepared in the course of his or her duties as a United States government employee.

[ ] The Author is a United States government employee but the Materials were NOT prepared in the course of his or her duties as a United States government employee.

ARTICLE AND VIDEO LICENSE AGREEMENT

1. **Defined Terms.** As used in this Article and Video License Agreement, the following terms shall have the following meanings: "**Agreement**" means this Article and Video License Agreement; "**Article**" means the article specified on the last page of this Agreement, including any associated materials such as texts, figures, tables, artwork, abstracts, or summaries contained therein; "**Author**" means the author who is a signatory to this Agreement; "**Collective Work**" means a work, such as a periodical issue, anthology or encyclopedia, in which the Materials in their entirety in unmodified form, along with a number of other contributions, constituting separate and independent works in themselves, are assembled into a collective whole; "**CRC License**" means the Creative Commons Attribution-Non Commercial-No Derivs 3.0 Unported Agreement, the terms and conditions of which can be found at: http://creativecommons.org/licenses/by-nc-nd/3.0/legalcode; "**Derivative Work**" means a work based upon the Materials or upon the Materials and other pre-existing works, such as a translation, musical arrangement, dramatization, fictionalization, motion picture version, sound recording, art reproduction, abridgment, condensation, or any other form in which the Materials may be recast, transformed, or adapted; "**Institution**" means the institution, listed on the last page of this Agreement, by which the Author was employed at the time of the creation of the Materials; "**JoVE**" means MyJove Corporation, a Massachusetts corporation and the publisher of The Journal of Visualized Experiments; "**Materials**" means the Article and / or the Video; "**Parties**" means the Author and JoVE; "**Video**" means any video(s) made by the Author, alone or in conjunction with any other parties, or by JoVE or its affiliates or agents, individually or in collaboration with the Author or any other parties, incorporating all or any portion of the Article, and in which the Author may or may not appear.

2. **Background.** The Author, who is the author of the Article, in order to ensure the dissemination and protection of the Article, desires to have the JoVE publish the Article and create and transmit videos based on the Article. In furtherance of such goals, the Parties desire to memorialize in this Agreement the respective rights of each Party in and to the Article and the Video.

3. **Grant of Rights in Article.** In consideration of JoVE agreeing to publish the Article, the Author hereby grants to JoVE, subject to **Sections 4** and **7** below, the exclusive, royalty-free, perpetual (for the full term of copyright in the Article, including any extensions thereto) license (a) to publish, reproduce, distribute, display and store the Article in all forms, formats and media whether now known or hereafter developed (including without limitation in print, digital and electronic form) throughout the world, (b) to translate the Article into other languages, create adaptations, summaries or extracts of the Article or other Derivative Works (including, without limitation, the Video) or Collective Works based on all or any portion of the Article and exercise all of the rights set forth in (a) above in such translations, adaptations, summaries, extracts, Derivative Works or Collective Works and(c) to license others to do any or all of the above. The foregoing rights may be exercised in all media and formats, whether now known or hereafter devised, and include the right to make such modifications as are technically necessary to exercise the rights in other media and formats. If the "Open Access" box has been checked in **Item 1** above, JoVE and the Author hereby grant to the public all such rights in the Article as provided in, but subject to all limitations and requirements set forth in, the CRC License.

612542.6   For questions, please contact us at submissions@jove.com or +1.617.945.9051.

4. **Retention of Rights in Article.** Notwithstanding the exclusive license granted to JoVE in **Section 3** above, the Author shall, with respect to the Article, retain the non-exclusive right to use all or part of the Article for the non-commercial purpose of giving lectures, presentations or teaching classes, and to post a copy of the Article on the Institution's website or the Author's personal website, in each case provided that a link to the Article on the JoVE website is provided and notice of JoVE's copyright in the Article is included. All non-copyright intellectual property rights in and to the Article, such as patent rights, shall remain with the Author.

5. **Grant of Rights in Video – Standard Access.** This **Section 5** applies if the "Standard Access" box has been checked in **Item 1** above or if no box has been checked in **Item 1** above. In consideration of JoVE agreeing to produce, display or otherwise assist with the Video, the Author hereby acknowledges and agrees that, Subject to **Section 7** below, JoVE is and shall be the sole and exclusive owner of all rights of any nature, including, without limitation, all copyrights, in and to the Video. To the extent that, by law, the Author is deemed, now or at any time in the future, to have any rights of any nature in or to the Video, the Author hereby disclaims all such rights and transfers all such rights to JoVE.

6. **Grant of Rights in Video – Open Access.** This **Section 6** applies only if the "Open Access" box has been checked in **Item 1** above. In consideration of JoVE agreeing to produce, display or otherwise assist with the Video, the Author hereby grants to JoVE, subject to **Section 7** below, the exclusive, royalty-free, perpetual (for the full term of copyright in the Article, including any extensions thereto) license (a) to publish, reproduce, distribute, display and store the Video in all forms, formats and media whether now known or hereafter developed (including without limitation in print, digital and electronic form) throughout the world, (b) to translate the Video into other languages, create adaptations, summaries or extracts of the Video or other Derivative Works or Collective Works based on all or any portion of the Video and exercise all of the rights set forth in (a) above in such translations, adaptations, summaries, extracts, Derivative Works or Collective Works and (c) to license others to do any or all of the above. The foregoing rights may be exercised in all media and formats, whether now known or hereafter devised, and include the right to make such modifications as are technically necessary to exercise the rights in other media and formats. For any Video to which this **Section 6** is applicable, JoVE and the Author hereby grant to the public all such rights in the Video as provided in, but subject to all limitations and requirements set forth in, the CRC License.

7. **Government Employees.** If the Author is a United States government employee and the Article was prepared in the course of his or her duties as a United States government employee, as indicated in **Item 2** above, and any of the licenses or grants granted by the Author hereunder exceed the scope of the 17 U.S.C. 403, then the rights granted hereunder shall be limited to the maximum rights permitted under such statute. In such case, all provisions contained herein that are not in conflict with such statute shall remain in full force and effect, and all provisions contained herein that do so conflict shall be deemed to be amended so as to provide to JoVE the maximum rights permissible within such statute.

8. **Protection of the Work.** The Author(s) authorize JoVE to take steps in the Author(s) name and on their behalf if JoVE believes some third party could be infringing or might infringe the copyright of either the Author's Article and/or Video.

9. **Likeness, Privacy, Personality.** The Author hereby grants JoVE the right to use the Author's name, voice, likeness, picture, photograph, image, biography and performance in any way, commercial or otherwise, in connection with the Materials and the sale, promotion and distribution thereof. The Author hereby waives any and all rights he or she may have, relating to his or her appearance in the Video or otherwise relating to the Materials, under all applicable privacy, likeness, personality or similar laws.

10. **Author Warranties.** The Author represents and warrants that the Article is original, that it has not been published, that the copyright interest is owned by the Author (or, if more than one author is listed at the beginning of this Agreement, by such authors collectively) and has not been assigned, licensed, or otherwise transferred to any other party. The Author represents and warrants that the author(s) listed at the top of this Agreement are the only authors of the Materials. If more than one author is listed at the top of this Agreement and if any such author has not entered into a separate Article and Video License Agreement with JoVE relating to the Materials, the Author represents and warrants that the Author has been authorized by each of the other such authors to execute this Agreement on his or her behalf and to bind him or her with respect to the terms of this Agreement as if each of them had been a party hereto as an Author. The Author warrants that the use, reproduction, distribution, public or private performance or display, and/or modification of all or any portion of the Materials does not and will not violate, infringe and/or misappropriate the patent, trademark, intellectual property or other rights of any third party. The Author represents and warrants that it has and will continue to comply with all government, institutional and other regulations, including, without limitation all institutional, laboratory, hospital, ethical, human and animal treatment, privacy, and all other rules, regulations, laws, procedures or guidelines, applicable to the Materials, and that all research involving human and animal subjects has been approved by the Author's relevant institutional review board.

11. **JoVE Discretion.** If the Author requests the assistance of JoVE in producing the Video in the Author's facility, the Author shall ensure that the presence of JoVE employees, agents or independent contractors is in accordance with the relevant regulations of the Author's institution. If more than one author is listed at the beginning of this Agreement, JoVE may, in its sole

ARTICLE AND VIDEO LICENSE AGREEMENT

jOVE
1 Alewife Center #200
Cambridge, MA 02140
tel. 617.945.9051
www.jove.com

discretion, elect not take any action with respect to the Article until such time as it has received complete, executed Article and Video License Agreements from each such author. JoVE reserves the right, in its absolute and sole discretion and without giving any reason therefore, to accept or decline any work submitted to JoVE. JoVE and its employees, agents and independent contractors shall have full, unfettered access to the facilities of the Author or of the Author's institution as necessary to make the Video, whether actually published or not. JoVE has sole discretion as to the method of making and publishing the Materials, including, without limitation, to all decisions regarding editing, lighting, filming, timing of publication, if any, length, quality, content and the like.

12. **Indemnification.** The Author agrees to indemnify JoVE and/or its successors and assigns from and against any and all claims, costs, and expenses, including attorney's fees, arising out of any breach of any warranty or other representations contained herein. The Author further agrees to indemnify and hold harmless JoVE from and against any and all claims, costs, and expenses, including attorney's fees, resulting from the breach by the Author of any representation or warranty contained herein or from allegations or instances of violation of intellectual property rights, damage to the Author's or the Author's institution's facilities, fraud, libel, defamation, research, equipment, experiments, property damage, personal injury, violations of institutional, laboratory, hospital, ethical, human and animal treatment, privacy or other rules, regulations, laws, procedures or guidelines, liabilities and other losses or damages related in any way to the submission of work to JoVE, making of videos by JoVE, or publication in JoVE or elsewhere by JoVE. The Author shall be responsible for, and shall hold JoVE harmless from, damages caused by lack of sterilization, lack of cleanliness or by contamination due to

the making of a video by JoVE its employees, agents or independent contractors. All sterilization, cleanliness or decontamination procedures shall be solely the responsibility of the Author and shall be undertaken at the Author's expense. All indemnifications provided herein shall include JoVE's attorney's fees and costs related to said losses or damages. Such indemnification and holding harmless shall include such losses or damages incurred by, or in connection with, acts or omissions of JoVE, its employees, agents or independent contractors.

13. **Fees.** To cover the cost incurred for publication, JoVE must receive payment before production and publication of the Materials. Payment is due in 21 days of invoice. Should the Materials not be published due to an editorial or production decision, these funds will be returned to the Author. Withdrawal by the Author of any submitted Materials after final peer review approval will result in a US$1,200 fee to cover pre-production expenses incurred by JoVE. If payment is not received by the completion of filming, production and publication of the Materials will be suspended until payment is received.

14. **Transfer, Governing Law.** This Agreement may be assigned by JoVE and shall inure to the benefits of any of JoVE's successors and assignees. This Agreement shall be governed and construed by the internal laws of the Commonwealth of Massachusetts without giving effect to any conflict of law provision thereunder. This Agreement may be executed in counterparts, each of which shall be deemed an original, but all of which together shall be deemed to me one and the same agreement. A signed copy of this Agreement delivered by facsimile, e-mail or other means of electronic transmission shall be deemed to have the same legal effect as delivery of an original signed copy of this Agreement.

A signed copy of this document must be sent with all new submissions. Only one Agreement is required per submission.

CORRESPONDING AUTHOR

Name: He Yan

Department: Institute of Nuclear and New Energy Technology

Institution: Tsinghua University

Title: Key procedures to optimize sealing process and achieve real time monitoring

Signature: He Yan

Date: 29-3-2019

Please submit a **signed** and **dated** copy of this license by one of the following three methods:
1. Upload an electronic version on the JoVE submission site
2. Fax the document to +1.866.381.2236
3. Mail the document to JoVE / Attn: JoVE Editorial / 1 Alewife Center #200 / Cambridge, MA 02140

Rebuttal letter

Dear Editors and Reviewers:

Thank you for your comments concerning our manuscript entitled "Key procedures to achieve sealing process and real time monitoring of glass-to-metal seal structure" (**ID: 60064**). Those comments are all valuable, very helpful for revising and improving our paper, as well as the important guiding significance to our researches.
We have made corrections according to your suggestions in the word file. The grammar typos and other mistakes have been improved. Thanks for your kind assistance.